Engineering Biomass into Formaldehyde-Free Phenolic Resin for Composite Materials

Yongsheng Zhang, Zhongshun Yuan, and Chunbao (Charles) Xu
Dept. of Chemical and Biochemical Engineering, Institute for Chemicals and Fuels from Alternative Resources (ICFAR), Western University, London, ON, Canada N6GA5B9

DOI 10.1002/aic.14716
Published online January 2, 2015 in Wiley Online Library (wileyonlinelibrary.com)

The use of formaldehyde to prepare phenol-formaldehyde (PF) resins is one of the primary challenges for the worldwide PF industry with respect to both sustainability and human health. This study reports a novel one-pot synthesis process for phenol-5-hydroxymethylfurfural (PHMF) resin as a formaldehyde-free phenolic resin using phenol and glucose, and the curing of the phenolic resin with a green curing agent organosolv lignin (OL) or Kraft lignin (KL). Evidenced by ^{13}C NMR, the curing mechanism involves alkylation reaction between the hydoxyalkyl groups of lignin and the ortho- and para-carbon of PHMF phenolic hydroxyl group. The curing kinetics was studied using differential scanning calorimetry and the kinetic parameters were obtained. The OL/KL cured PHMF resins were tested in terms of thermal stability, and mechanical properties for their applications in fiberglass reinforced composite materials. The results obtained demonstrated that OL/KL can be promising curing agents for the PHMF resins. © 2015 American Institute of Chemical Engineers *AIChE J*, 61: 1275–1283, 2015

Keywords: formaldehyde-free, sustainable phenolic resin, curing kinetics, lignin, fiberglass reinforced composite materials

Introduction

Phenol-formaldehyde (PF) resin,[1] the first commercial synthetic resin, has been widely used in a variety of commercial applications owing to its superior dimensional stability, moisture resistance, strength, and high glass transition temperature (T_g).[2,3] However, the increased environmental awareness and stringent environmental laws underscores the need for the development of sustainable phenolic resin for environmental benefits. Many manufacturers are now looking for "greener" and more environmentally friendly alternatives to synthetic materials.[4]

Biomass, mainly composed of lignin, cellulose (CEL), and hemicellulose, is the primary feedstock for the production of renewable chemicals.[5,6] Lignin,[7] tannin,[8] and cardanol[9] have been used as substitutes for petroleum-based phenol. However, formaldehyde, a carcinogenic compound suggested by the U.S. Occupational Safety and Health Administration,[10–12] have not been paid enough attention yet. Glucose is plentifully available by hydrolysis of CEL and hemi-cellulose that are two main components in biomass.[13–17] Thus, developing bio-based alternative (such as hydroxymethylfurfural [HMF]—a derivative of glucose) to formaldehyde as a feedstock for the synthesis of phenolic resins is of great significance.[18] HMF is structurally combined with furfural and hydroxymethyl furan, and furfural is known to react with phenol[19] to form phenolic polymers. HMF is thus a potential substitute for formaldehyde in synthesizing phenolic resin and producing phenol-5-hydroxymethylfurfural (PHMF) resin—a green alternative to conventional PF resins. Our research group has successfully developed a one-pot process to synthesize PHMF resin with high conversion which is submitted for publication.

Furthermore, hexamethylene tetramine (HMTA), the most common compound currently used for curing of Novolac-type phenolic resins, is also among the chemicals with environmental concerns as it could decompose into ammonia and formaldehyde even at room temperature.[20–22] Thus, HMTA is classified as a hazardous air pollutant per the U.S. Federal Environmental Protection Agency.[23] Therefore, replacing HMTA with more environmentally friendly curing agents has become an important subject.

Simitzis et al. produced Novolac-type PF resins (Figure 1) cured with mixture of HMTA and one of the following components: the olive residue after separation of olive oil, Kraft lignin (KL), hydroxymethylated Kraft lignin, and CEL. It was found that although activation energy (E_a) and pre-exponential constant (k) varied with different cross-linkers, the reaction order n is approximately the same ($n \cong 1$). However, the mechanisms of the cross-linking reactions have not yet been discussed and reported.[24]

In a literature work by Sergeev et al.,[25] 2,6-di (hydroxymethyl)-*p*-cresol, 3,3′,5,5′-tetra (hydroxymethyl)-4,4′-isopropylidenediphenol, and 2,6-bis(2-hydroxy-3-hydroxymethyl-5-methylbenzyl)-4-methylphenol (Figure 2) were tested as curing agents for Novolac resins. However, these chemicals are all expensive and not feasible for industrial applications. Lignin with hydroxymethyl group[7] and similar structure to

Correspondence concerning this article should be addressed to Z. Yuan at zyuan25@uwo.ca or C. (Charles) Xu at cxu6@uwo.ca.

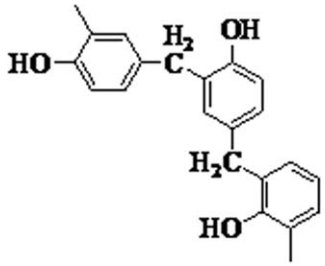

Figure 1. General structure of a novolac resin.

the above phenolic compounds is supposed to be a suitable bio-based substitute for HMTA as the industrial curing agent for Novolac phenolic resin.[26] However, to the best of our knowledge, there is few research regarding curing of phenolic resins with lignin so far. Organosolv lignin (OL) is obtained from wood or other lignocellulosic biomass by extraction with various organic solvents.[27] KL is the by-product generated at a large amount worldwide (estimated at 50 million tons annually) from the Kraft pulping process. Currently, KL is mainly utilized as a low-value fuel in recovery boilers in Kraft pulp mills for process heat generation and pulping chemicals recovery. More valuable applications of KL for chemicals are of great significance and interest not only to pulp mills for better economy but also to the chemical industries for feedstock sustainability.

The main objectives of this work herein are to characterize PHMF resin synthesized with glucose-derived HMF as sustainable substitute for formaldehyde and to realize the curing of PHMF with OL or KL as a novel curing agent. The synthesized PHMF resin was characterized for its curing characteristics, thermal behavior, and mechanical properties while being utilized as a polymer matrix for composite materials. For comparison, the Novolac PHMF resin was cured with HMTA and characterized under the same conditions.

Materials and Methods

Materials

Dimethyl sulfoxide, tetrahydrofuran (THF), and acetone were obtained from Fisher Scientific and were used as received. Glucose, phenol, chromium (II) chloride ($CrCl_2$), chromium (III) chloride ($CrCl_3$), tetraethylammonium chloride (TEAC), 1, 4-benzenedimethanol (BDM), and hexamethylenetetramine (HMTA) were purchased from Sigma-Aldrich and used as received. OL with $M_w = 2600$, PDI = 3.6 and KL with $M_w \cong 10{,}000$, PDI $\cong$ 2 were supplied by Lignol and FPInnovations, respectively, and used without further treatment. BGF fibreglass cloth was purchased from Freeman, OH.

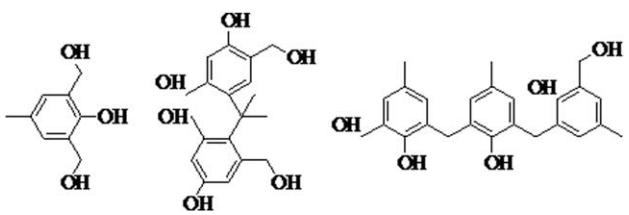

Figure 2. Structures of curing agents used in reference 25.

Synthesis of Novolac PHMF resin

The PHMF resin was synthesized with a one-pot synthesis protocol as briefly described here. In a batch reactor (a 100 mL glass pressure reactor equipped with a magnetic stir bar and a Teflon stopper), 0.0837 g $CrCl_2$, 0.0907 g $CrCl_3.6H_2O$, and 0.3739 g TEAC were added as catalyst along with 7.05 g phenol (0.075 mol), 27.00 g (0.150 mol) glucose, and 6.00 g water. The reactor was heated to 120°C for 8 h. The mixture turned to green initially while as the reaction progressed more glucose dissolved into the liquid phase and the admixture became black. The reaction mixture was cooled to room temperature, diluted, and analyzed with high performance liquid chromatography (HPLC) to determine free phenol and glucose contents.

After the PHMF resin was prepared and water was removed, it was first dissolved in acetone to separate unreacted glucose. The solvents including the unreacted phenol were removed by rotary evaporation and the product was dried in a vacuum oven under 60°C overnight.

Product analysis

The FTIR spectra were obtained with a Nicolet 6700 Fourier Transform Infrared Spectroscopy with smart ITR/ATR accessory, scanning from 500 to 4000 cm^{-1}.

^1H nuclear magnetic resonance (NMR) and ^{13}C NMR spectra were acquired using a Varian Inova 600 NMR (16–32 scans at 298 K) spectrometer equipped with a Varian 5 mm triple-resonance indirect-detection HCX probe. A 2 s recycle delay, 3.6 s acquisition time, a 45-degree tip angle (pw = 4.8 μs), and a spectral width from 0 to 14 ppm (sw = 9000.9 Hz) were used. Two-dimensional (2-D) NMR spectra (COSY and HMQC) were obtained using standard Bruker pulse programs. D_6-DMSO was selected as the solvent of the resin and fine power was used for solid-state (cured resin) cross-polarization magic-angle spinning ^{13}C NMR.

HPLC analysis was conducted with Waters Breeze instrument (1525 binary pump with refractive index and ultraviolet detector). Glucose and phenol contents were analyzed using Bio-Rad Aminex HPX-87H column and HPLC grade 0.005 M H_2SO_4 water as the mobile phase (flow rate 0.6 mL/min).

Molecular weights were measured on a Waters Styrylgel HR1 gel permeation chromatography (GPC, 1525 binary pump, UV detector set at 270 nm, Waters Styragel HR1 column at 40°C) using THF as the eluent at a flow rate of 1 mL/min and linear polystyrene as standards for calibration.

The thermal curing properties of the resins were evaluated with a differential scanning calorimetry (DSC, Mettler-Toledo, Switzerland) under 50 mL/min N_2 at heating rate of 10°C/min between 40 and 250°C in an aluminum crucible.

Thermal stability of the uncured and cured PHMF resin was measured using a TGA 2050 (Thermogravimetric Analyzer, TA Instruments). Approximately 10 mg of sample was placed in a platinum pan and heated to 700°C at 10°C/min in a nitrogen atmosphere of 50 mL/min. Thermomechanical properties of the cured woven fibreglass cloth-PHMF composites were measured using dynamic mechanical analysis (DMA) and universal testing machine. The composites were formulated by mixing woven fibreglass cloth and matrix (PHMF resin + curing agent) at a ratio of 1:1 (wt/wt). Prior to compounding, the PHMF resin and the curing agent were first dissolved in acetone to form a homogeneous admixture

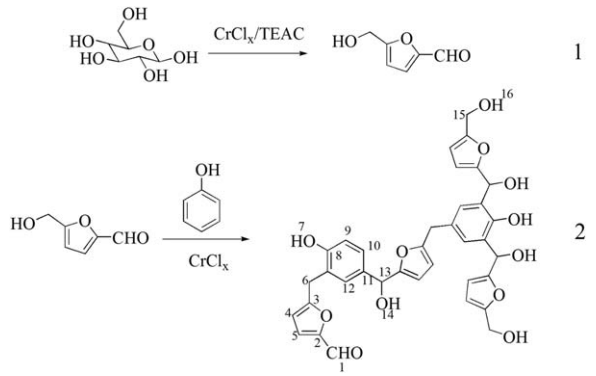

Scheme 1. Reaction mechanism of *in situ* generated HMF from glucose (1) and the synthesis of phenol-HMF (PHMF) resin (2).

and the acetone was removed by vacuum under 50°C. The amounts of the curing agents were controlled at 20 wt % and 15 wt % of the bulk resin for OL/KL and for HMTA,[28] respectively. Carver (hydraulic unit model 3925) hot press was used for composites fabrication. Fibreglass reinforced composites were prepared by lay up method using BGF fiberglass cloth and PHMF resin in a hot press under 5000 psi pressure with a curing procedure of 120°C for 30 min, 150°C for 30 min, and 180°C for 1 h. The cured composites were cut into rectangular samples with approximate dimensions of 20 × 10 × 1 mm^3, which were tested using a Netzsch 242C DMA in three point bending geometry, at a driving frequency of 1 Hz with a deflection of 5 μm and the temperatures ramped from 30 to 250°C at a scanning rate of 5°C/min. The pressed composites were also shaped into dumbbell-shaped samples and their tensile strengths were measured in accordance to ASTM 638 on an ADMET Expert 7600 universal test machine.

Results and Discussion

Characterizations of the PHMF resin

The PHMF resin obtained was dark solid. Free phenol and glucose contents in the product mixture were determined to be 8.5 wt % and 12 wt %, respectively, by HPLC analysis. ^{1}H NMR spectrum of the purified PHMF resin shows the following chemical shifts: 9.5 ppm (s, CHO), 7.3–6.3 ppm (m, aromatic), 3.9 ppm (s, benzyl CH_2), and 2.3 ppm (s, CH). FT-IR spectra of the PHMF resin gives the absorbance peaks (cm^{-1}) at 1012 (C-OH, aliphatic), 1226 (C—O, aromatic), 1600–1400 (C—C, aromatic), 1702 (CHO), 2910 (CH_2), 3275 (OH). The presence of benzyl CH_2 function group could be the evidence of the reaction between phenol and HMF (*in situ* converted from glucose).

Here, $CrCl_x$ catalyze both the HMF formation reaction[29,30] and the resinification reaction of HMF with phenol. This reaction mechanism is proposed by Scheme 1. Glucose is first isomerized to fructose which is subsequently dehydrated to HMF in first step.[31,32] The reaction is followed by nucleophilic addition of the electron rich carbons of the *para*- and *ortho*-positions of phenol to the electrophilic aldehyde group in HMF. The hydroxymethyl group in HMF can simultaneously react with the *para*- and *ortho*-position of phenol OH through a Friedel-Crafts alkylation. However, there might be very little side reactions such as glucose conversion into humin which is incorporated into resin or connection between glucose aldehyde and phenol. The synthesized PHMF resin has a number average molecular weight (M_n) of 765 g/mol and a weight average molecular weight (M_w) of 1850 g/mol, which evidences the successful resinification of phenol with HMF formed in the process. For better understanding of reaction mechanism and comparison with 2-D NMR spectrum, the corresponding NMR spectrum peak assignments are summarized in Table 1.

In ^{1}H NMR COSY spectra of PHMF resin (Figure 3), the presence of off diagonal cross peaks from protons at δ 6.7/7.1 indicates the coupling of H^4/H^5 while the existence at δ 6.4/7.4 is from H^9/H^{10}. The very minor cross peaks at δ 2.4/2.8 indicates the anti-geometry of protons H^{13}/H^{14} and H^{15}/H^{16} (methylene and hydroxyl). The absence of cross peaks from the protons methylene/*para*-substituted phenol (H^{11}/H^{13}) indicates the connection between HMF and *para*-phenol in the resins.

The above discussion can be affirmed by observation with the ^{1}H-^{13}C NMR-HSQC spectra of PHMF (Figure 4). The crosspeaks at δ 9.4/178 ppm are due to H^1/C^1 signals of aldehyde in HMF. Two dominant H/C crosspeaks, δ 7.0/131 ppm from H^{10}/C^{10} signals of the meta- unsubstituted phenol and δ 6.7/115 of aromatic proton (H^4/C^4 and H^5/C^5) from HMF were observed. The high density of the crosspeaks at δ 6.7/115 is consistent with high fractions of aromatics in PHMF structure (Scheme 1). The H/C signals of hydroxyl substituted methylene group (H^{14}/C^{13}) could be identified at δ 4.5/57 ppm.

Effects of the amounts of curing agents on glass transition temperature

The glass transition temperature (T_g) establishes the temperature below which the resin is safely used, and thus, it is believed to be an important parameter of polymeric and composite materials. There have been many methods

Table 1. ^{1}H NMR and ^{13}C NMR Spectrum Peak Assignments

^{1}H NMR		^{13}C NMR	
Shift (ppm)	Peak Assignment	Shift (ppm)	Peak Assignment
9.5	CHO 1	178	Aldehyde carbon 1
8.3	OH of phenol 7	162	*o*-carbon of the furan 2, 3
7.3–6.3	Aromatic 4, 5, 9, 10, 12	156, 157	Hydroxyl substituted phenolic carbons, 8
4.5	CH 13	152	Carbon adjacent to oxygen and aldehyde group of the furan ring, 2
3.9	benzyl CH_2 6		
2.5	DMSO	131	*m*-carbon of unsubstituted phenol, 10
2.3	OH 14		
		119	*m*-carbon of furan, 4, 5
		115	*o*-carbon on phenolic ring, 9
		57	C of methylene/methine, 13, 15

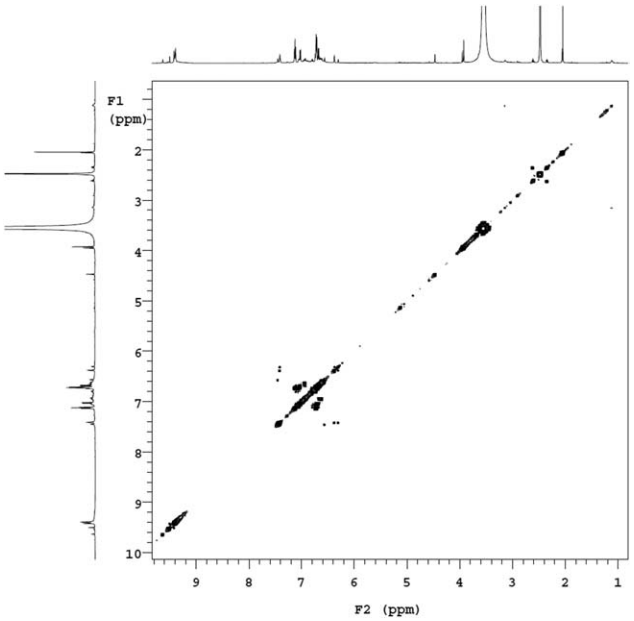

Figure 3. ^{1}H-^{1}H NMR-COSY spectrum of PHMF resin.

developed in determining T_g in polymer systems.[33] Here, the T_g was estimated by the midpoint of an endothermic step of cured resin in the DSC profile. Neat resin was cured with OL and KL, respectively, with four varying amounts of curing agents: 10 wt %, 20 wt % 30 wt %, and 40 wt %. As presented in the Table 2, the T_g values range from 110 to 135°C, reaching maximum at 20 wt % of the cross-linkers. Low amount (10 wt %) of OL/KL is not sufficient for cross-linking of the resin, but high addition amounts, 30 wt % and 40 wt %, of OL/KL resulted in reduced T_g. Thus, the optimal ratio of curing agent was determined to be 20 wt % of the resin. The PHMF resin cured with OL/KL has a similar T_g with PF Novolac resins, which was reported to be 134°C.[34]

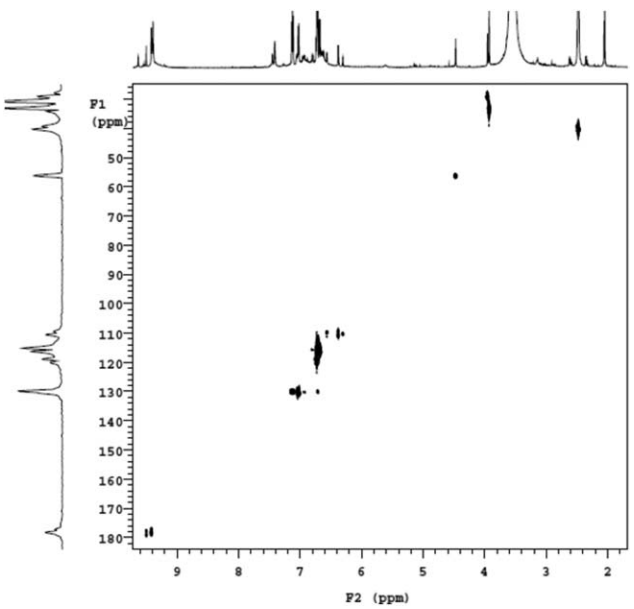

Figure 4. ^{1}H-^{13}C NMR-HSQC spectrum of PHMF resin.

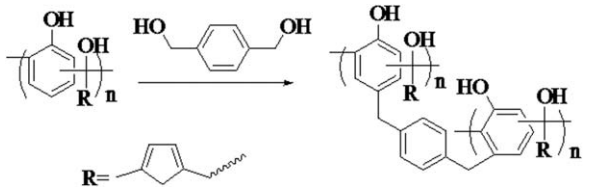

Scheme 2. Proposed curing reaction mechanism for PHMF novolac with OL/KL.

Table 2. Glass Transition Temperature of PHMF Resin Cured with OL/KL at Various Addition Amounts

Sample PHMF + OL (wt %)	T_g (°C)	Sample PHMF + KL (wt %)	T_g (°C)
10	120	10	119
20	133	20	128
30	130	30	125
40	120	40	123

Curing mechanism

One objective of this article is to identify the reaction occurring in PHMF/OL(KL) systems and to analyze their effects on properties of the harden materials. However, hydroxymethylene group might be formed on curing whereas it also exists in OL/KL. To lower this complexity, BDM was used as a model compound for OL/KL to study the curing mechanism of the PHMF resin.

The monitoring along the curing process by FTIR spectroscopy (Figure 5) presents that hydroxyl group of BDM almost disappeared after curing of the PHMF resin with 20 wt % addition of BDM. The functional groups taking part in the curing process was confirmed by the formation of CH_2 groups and their stretching vibration band at 2978 cm^{-1}. Further, the absorbance at 3652 cm^{-1} represents the phenolic hydroxyl group without hydrogen bonding effects due to the restricted structure after curing.

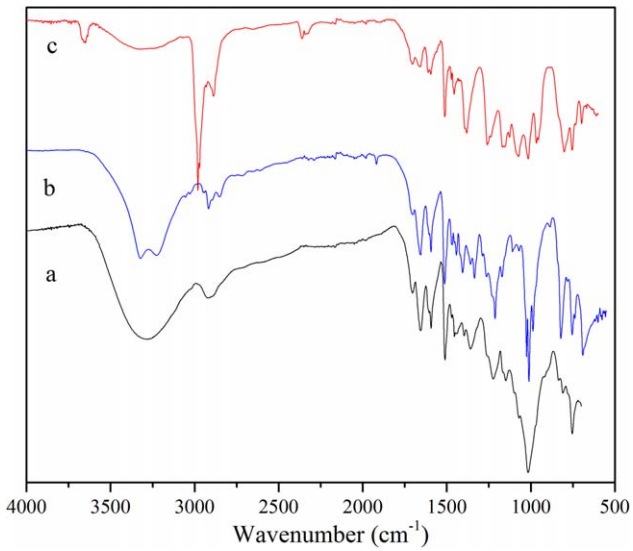

Figure 5. FTIR spectra of PHMF resin (a), admixture of PHMF with 20 wt % BDM before curing (b), and cured PHMF with 20 wt % BDM (c).

[Color figure can be viewed in the online issue, which is available at wileyonlinelibrary.com.]

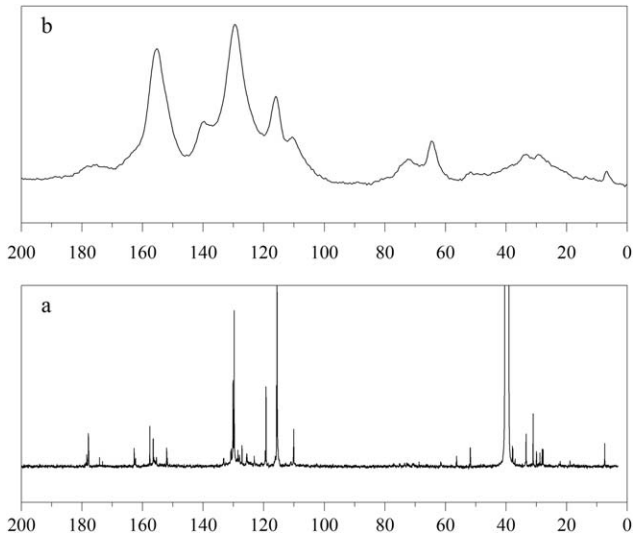

Figure 6. ^{13}C NMR spectra of PHMF (a) and cured PHMF with 20 wt % 1, 4-BDM (b).

The carbon (^{13}C) NMR spectra in Figure 6 indicate key disparities of the neat PHMF resin and the cured resin with BDM. It is noted that the peak corresponding to unsubstituted aromatic carbon at the *para*-position in the PHMF resin (119 ppm) disappeared, suggesting some group attached to this *para*-phenolic carbon. While the formation of substituted *para*-phenolic carbon (139 ppm) after curing implies that hydroxyl group from the model compound reacted with PHMF. One possible explanation to these findings could be the alkylation reaction of PHMF and BDM catalyzed by chromium chloride.[35] Based on the above analysis, the curing mechanism for PHMF Novolac with OL/KL is proposed and depicted in Scheme 2. On another note, some peaks detected at 72 and 64 ppm can be assigned to hydroxymethylene functional groups, suggesting some unreacted BDM.

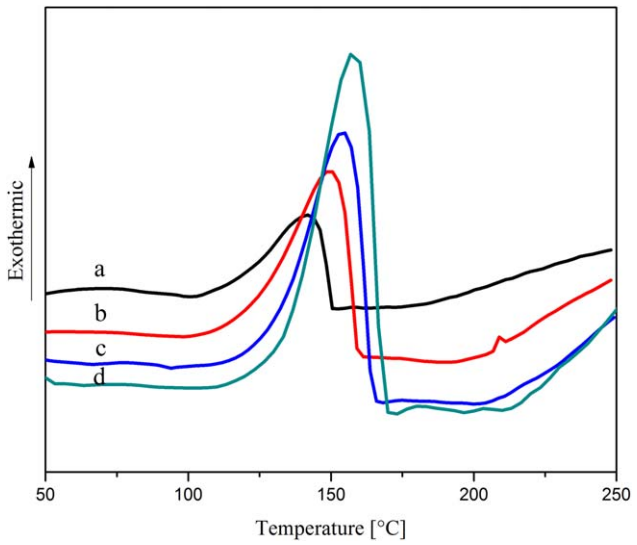

Figure 7. Heat release vs. temperature in curing of PHMF resins with OL at: 5°C/min (a), 10°C/min (b), 15°C/min (c), and 20°C/min (d).

[Color figure can be viewed in the online issue, which is available at wileyonlinelibrary.com.]

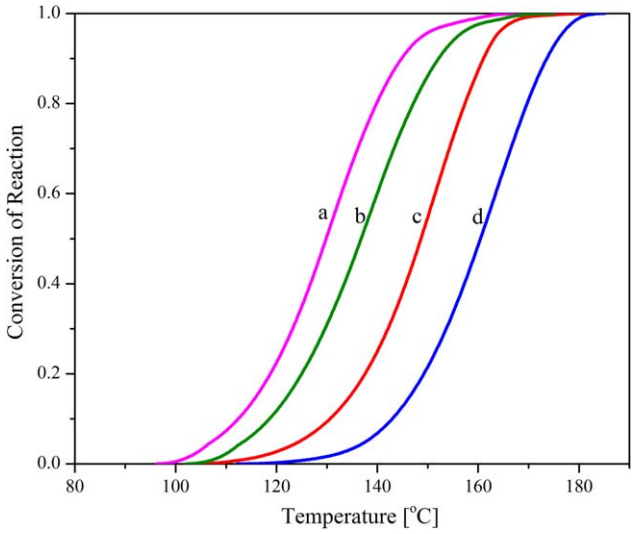

Figure 8. Curing reaction conversion vs. temperature at: 5°C/min (a), 10°C/min (b), 15°C/min (c), and 20°C/min (d).

[Color figure can be viewed in the online issue, which is available at wileyonlinelibrary.com.]

Curing kinetics

The properties of cured resin are significantly dependent on the extent of cure and explicit knowledge of the cross-linkage behavior. Curing kinetics of the PHMF resins with OL/KL or HMTA are thus studied using dynamic DSC, as was reported in the literature.[36] Similar to the sample preparation for DMA tests, the PHMF resin and the curing agents were first formed a homogeneous admixture.

In recent decades, processing of thermosetting resins has received increasing attention from the automotive, aerospace, and construction industries. Processing of these materials is important and the understanding of curing kinetics is herein essential in the design of the operation conditions. Among current analytical methods, dynamic DSC measurements

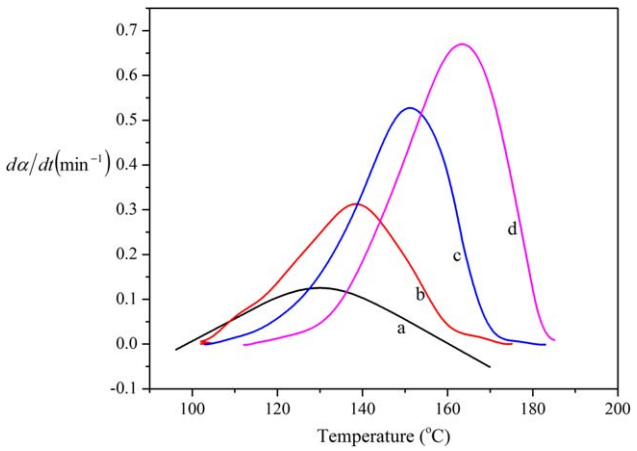

Figure 9. Curing reaction rate against temperature at: 5°C/min (a), 10°C/min (b), 15°C/min (c), and 20°C/min (d).

[Color figure can be viewed in the online issue, which is available at wileyonlinelibrary.com.]

Table 3. Kinetics Data for Curing PHMF Resin with 20 wt % OL

Heating rate (°C/min)/ Peak Temperature (°C)/ E_a (kJ/mol) by Freeman–Carroll				Kissinger		FWO	Crane
				E_a (kJ/mol)	A	E_a (kJ/mol)	n
5	10	15	20				
142.30	149.59	154.62	157.84				
61.49	118.13	139.02	127.07	124.88	2.244 E + 12	125.44	0.95

were commonly conducted. In this work, curing kinetics of PHMF resins was investigated with proper amount of OL as a lignin representative.

DSC curves of PHMF resins with OL at varying heating rates (5°C/min, 10°C/min, 15°C/min, and 20°C/min) are illustrated in Figure 7. The DSC curves imply that the curing reaction occurs at around 150°C. As the heating rate increases, a higher curing peak temperature was observed. A possible reason is that the active groups in the resin react with each other at a lagged temperature at an increased ramping rate. The partially cured system will have higher activation energy because of the increased steric hindrance that reduces the accessibility of the curing agent to the resin.

The curing reaction conversion as per their individual temperature range is given by integrating heat release curves (Figure 8). The S shape conversion represents the shift to higher temperature range along with increased ramp rate. The conversion is further differentiated to get the reaction rate profiles (Figure 9). A higher curing reaction rate and a higher curing peak temperature were achieved at a higher ramping rate, which could be attributed to the favorable effect of temperature as the reaction proceeds.

Specifically, kinetic parameters are determined by the following classic models:

***Freeman–Carroll method*[37]**

$$\Delta\ln(d\alpha/dt)/\Delta\ln(1-\alpha)=n-(E_a/R)\Delta(1/T)/\Delta\ln(1-\alpha) \quad (1)$$

At a certain heating rate, a straight line could be obtained when plotting $\Delta\ln(d\alpha/dt)/\Delta\ln(1-\alpha)$ against$\Delta(1/T)/\Delta\ln(1-\alpha)$. The values of E_a can be taken from the slope.

***Kissinger model*[38]**

$$E_a\beta/(RT_p^2)=Ae^{-E_a/(RT_p)} \quad (2)$$

where β is the heating rate, expressed by $\beta=dT/dt$. By taking the logarithm of Eq. 2, one has Eq. 3. A and E_a can be obtained by plotting $-\ln(\beta/T_p{}^2)$ vs. $1/T_p$, where T_p is the peak curing temperature

$$-\ln(\beta/T_p{}^2)=-\ln\left(\frac{AR}{E_a}\right)+\left(\frac{1}{T_p}\right)\left(\frac{E_a}{R}\right) \quad (3)$$

***Flynn–Wall–Ozawa model (Eq. 4)*[39,40]**

$$\log\beta=-\frac{0.4567E_a}{RT_p}+C \quad (4)$$

If one plots $\log\beta\sim 1/T_p$, the slope is $-\frac{0.4567E_a}{R}$

***Crane model (Eq. 5)*[41]**

If one plots $\ln\beta\sim 1/T_p$, the reaction order n can be obtained by the slope: $-\frac{E_a}{nR}$

$$\frac{d(\ln\beta)}{d(1/T_p)}=-\frac{E_a}{nR} \quad (5)$$

The kinetics parameters were calculated as per Eqs. 1–5 and are summarized in Table 3. Interestingly, E_a obtained by Freeman–Carroll method was found to increase significantly with the scanning rate, implying strong dependence of curing kinetic parameters on the heating rate. It is also speculated that 5°C/min allowed the functional groups with enough time for diffusion. The lower steric hindrance through the curing process gave lower activation energy.

As a reference, the curing experiments of PHMF resin with the conventional Novolac resin curing agent HMTA were conducted, and the DSC curves are illustrated in Figure 10. The kinetics parameters from the experiments are presented in Table 4. Comparing the kinetics results in Tables 3 and 4, the calculated activation energy is 113 kJ/mol and 125 kJ/mol for PHMF resin cured with 15 wt % HMTA and 20 wt % OL, respectively. It is thus clear that the PHMF resin could be cured more easily with HMTA than with OL, likely due to the greater steric structure and lower reactivity of OL.

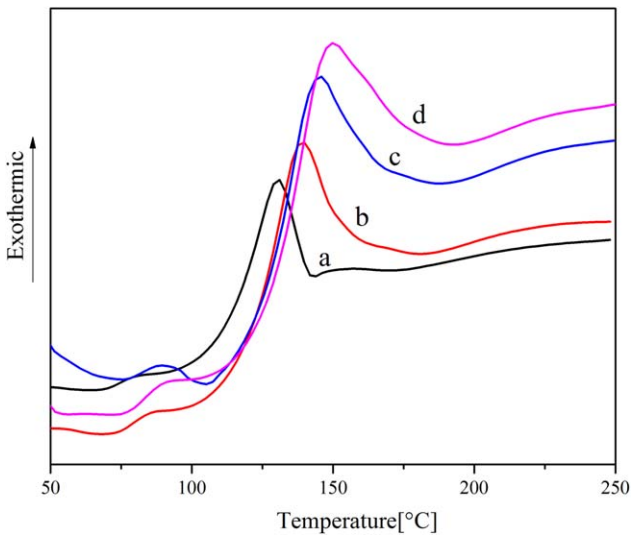

Figure 10. DSC spectra of the PHMF resin cured with HMTA at various heating rates: 5°C/min (a), 10°C/min (b), 15°C/min (c), and 20°C/min (d).

[Color figure can be viewed in the online issue, which is available at wileyonlinelibrary.com.]

Table 4. Kinetics Data for Curing PHMF Resin with 15 wt % HMTA

Peak Temperature (°C)				Kissinger		FWO	Crane
Heating Rate (°C/min)							
5	10	15	20	E_a (kJ/mol)	A	E_a (kJ/mol)	n
131.59	139.12	143.90	148.17	112.69	1.49 E + 11	113.69	0.95

Thermal stability

TGA experiments were performed to evaluate the thermal stability of the PHMF resins harden with OL/KL/HMTA and Figure 11 displays their thermograms. From the TGA data, thermal stability factors, including the initial decomposition temperature, T_5 (the temperature at 5% weight loss), the temperature at 50% weight loss, $T_{50\%}$, the temperature at the maximum decomposition rate, T_{max}, and the residual mass at 700° were obtained and are presented in Table 5. The results show that the cured PHMF polymer is thermally stable up to about 220–240°C (the T_5). The T_{max} for the OL-cured ($T_{max} = 397$°C) and the KL-cured PHMF ($T_{max} = 407$°C) is almost 100°C higher than that cured with HMTA.

In addition, from Figure 11 all cured PHMF resins exhibited a sharp thermal decomposition behavior between 250°C and 500°C, as similarly observed by other researchers in cured PF resins[42] and in lignin substituted lignin-PF resins.[7] The fast decomposition is believed to be resulted from pyrolytic degradation of the resins, involving fragmentation of alkyl linkages, releasing monomeric/oligomeric phenolic compounds into the vapour phase. Since ammonia decomposed from HMTA would form C—N bond which is less strong, some harden resin may be broken into smaller fractions at a lower temperature, comparing with those resin cured with an agent (such as OL and KL) of a larger molecular weight. Interestingly, the yields of solid residue from all samples with different curing agents at 700°C were within a narrow range (43–47 wt %), suggesting similar thermal stability at high temperatures.

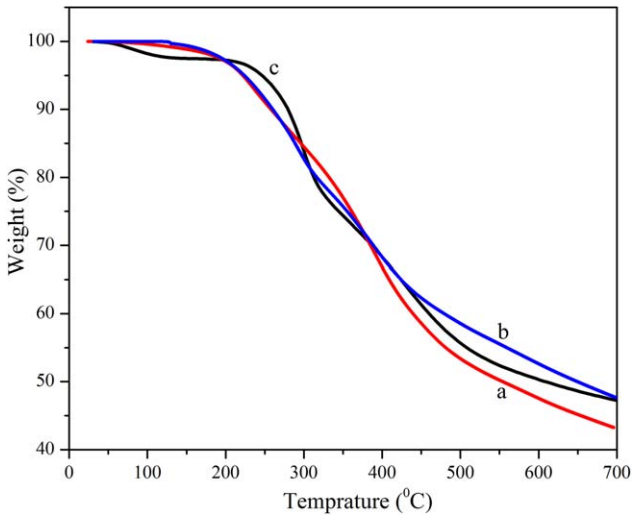

Figure 11. Thermal stability of PHMF resin cured with OL(a)/KL(b) and its comparison with that cured by HMTA(c).

[Color figure can be viewed in the online issue, which is available at wileyonlinelibrary.com.]

Thermomechanical properties of fiberglass reinforced biocomposites using PHMF resin

Another objective of this work is to utilize the PHMF resin as a polymer matrix of fiberglass reinforced biocomposites. The biocomposites were prepared by hand layup impregnation of the fibers with the PHMF resin cured on a hot-press. The preparation method was detailed previously in the section of "Materials and Methods."

The DMA profiles of cured biocomposites are illustrated in Figure 12, where the storage modulus (E') and tan δ are plotted against temperature. Storage modulus, representing the stiffness of a cured resin, is proportional to the energy stored during a loading cycle. The T_g of the cured biocomposite samples in this study was determined by the peak temperature of individual plot of tan δ. As we know, different T_g values of the thermosetting resins reflect different crosslink densities. The width of the tan δ peak reflects polymer network heterogeneity, and a broader peak implies a more heterogeneous polymer. From Figure 12, the T_g value of the biocomposite cured with OL is around 267°C, very close to that with HMTA (280°C). Although the biocomposite cured with KL presented a lower T_g (220°C) compared with those with OL and HMTA, it is still approximately 130°C higher than that of a cardanol-formaldehyde phenolic resin-based composite.[43] More work is on-going in the authors' group to investigate on the mechanical properties to further increase the glass transition temperatures and lower the curing temperatures of the PHMF-based biocomposites.

To investigate the effect of various curing agents: OL, KL, and HMTA on the mechanical properties of the resulting resins, Eq. 6 is used to calculate the crosslink density of the cured systems

$$E = 3v_eRT \tag{6}$$

The storage modulus (E) obtained from DMA is similar in value to the elastic modulus (E) at temperatures well above T_g, and therefore, E can be considered to be equivalent to the storage modulus at T_g. v_e is the crosslink density, calculated from Eq. 6, whose values were given previously in Table 5, R is the gas constant and T is the temperature in Kelvin. From the Eq. 6, E is proportional to v_e, suggesting that a higher crosslink density is corresponding to a larger storage modulus (E). The crosslink densityv_e for the

Table 5. Thermomechanical Properties of the Cured PHMF Resin with Various Curing Agents

Hardener	T_5 (°C)	T_{max} (°C)	T_{50} (°C)	700°C wt %	T_g (°C)[a]	v_e[b]/10^4(mol m^3)
OL	222	397	555	43.26	267	4.28
KL	224	407	650	47.61	220	1.65
HMTA	238	298	607	47.15	280	4.14

[a]Glass transition temperature determined by DMA.
[b]Crosslink density.

composite is calculated and presented in Table 5. It can be seen that v_e of PHMF/OL is similar with PHMF/HTMA system, but the PHMF/KL resin presents a little lower value of v_e. The reason might be that KL with high molecular weight contains less reactive hydroxymethylene groups, hence leading to a lower crosslink density (storage modulus) than OL.

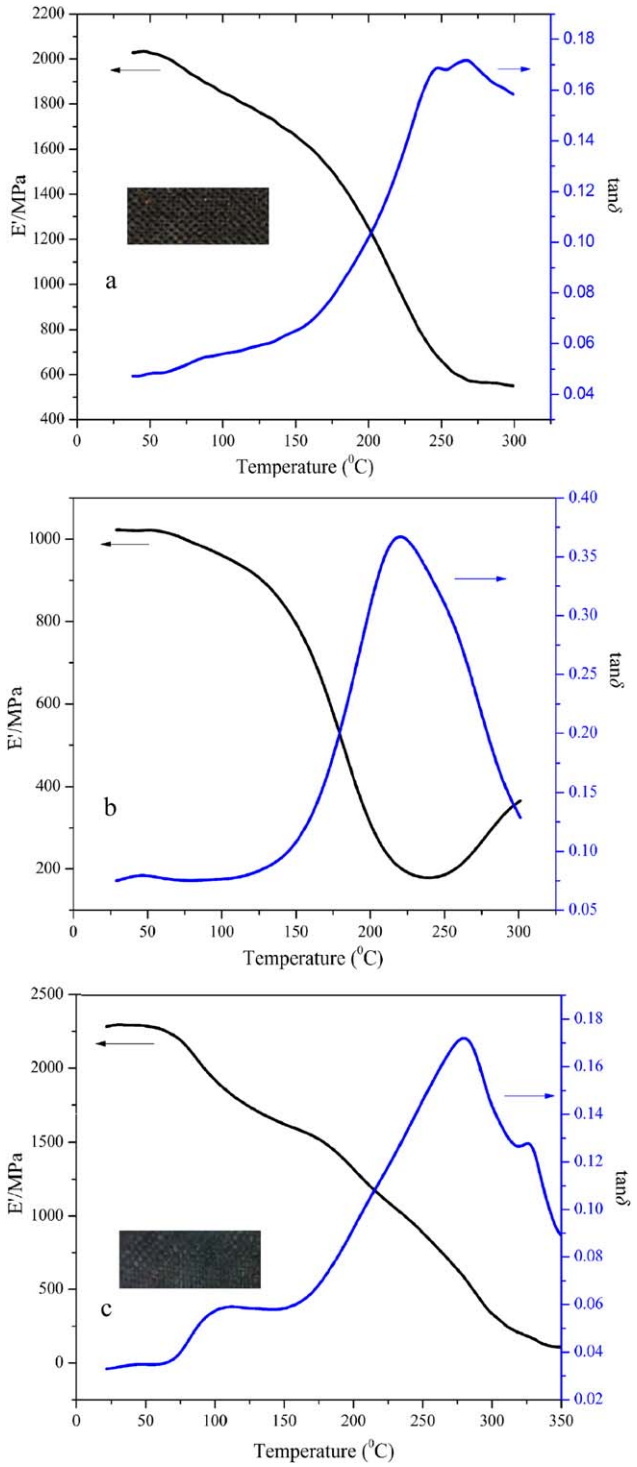

Figure 12. DMA profiles of the *woven fiberglass cloth-PHMF resin composites* cured with OL (a), KL (b), and HMTA (c).

[Color figure can be viewed in the online issue, which is available at wileyonlinelibrary.com.]

Table 6. Tensile Strengths of Woven Fiberglass Cloth-PHMF Resin Composites Cured with Various Curing Agents

Sample	Tensile Strength
PHMF + OL	99 ± 5 MPa
PHMF + KL	93 ± 2 MPa
PHMF + HMTA	109 ± 4 MPa

Table 6 gives the comparison of the tensile strengths of woven fiberglass cloth-PHMF resin composites cured with OL/KL compared with that of the composites cured with a commercial curing agent (i.e., HMTA). The OL/KL cured composites have tensile strengths of around 95 MPa, with a 10% inferior to that of the HMTA cured composite. These are actually comparable to phenolic sheet moulding composite which has a tensile strength of 96 MPa.[44] The tensile strength of the long glass fiber reinforced PF resin molding compounds was reported to be 115 MPa,[44] comparable to the values obtained in this work for the PHMF-based composites. Interestingly, the woven fiberglass cloth-PHMF resin composites cured with OL/KL are likely stronger than banana fibres/PF composites (28 MPa)[45] and sisal fibre/PF composites (60 MPa).[46]

Conclusions

In this work, HMF was *in situ* generated from glucose using chromium chlorides as catalysts and was polymerized with phenol to produce a Novolac PHMF resin. The structure was identified and the possible reaction schemes were proposed and discussed. Curing of the PHMF was realized using formaldehyde-free curing agents including OL or KL, starting at 120°C and peaked at around 150°C. The curing kinetic parameters for the PHMF resin were calculated. The curing mechanism was elucidated using FTIR and ^{13}C NMR. The resin was successively applied as polymer matrix in fiberglass to produce biocomposites with good thermomechanical property. The PHMF resin has a glass transition temperature of 120–130°C, and the fiberglass reinforced biocomposites using PHMF resin hardened with OL/KL has a T_g up to approximately 270°C, which is similar to those of the HMTA-cured PF resin. The lignin (OL/KL) cured woven fiberglass cloth-PHMF resin composites demonstrated comparable tensile fracture strengths (~95 MPa) to that of the HMTA cured composite.

Acknowledgments

The authors are grateful for the financial support from NSERC/FPInnovations Industrial Research Chair Program in Forest Biorefinery and the Ontario Research Fund-Research Excellence (ORF-RE) from Ministry of Economic Development and Innovation, as well the Mitacs internship award. Support from the industrial partners including FPInnovations, Arclin Canada, BioIndustrial Innovation Centre, and CENNATEK is also acknowledged.

Literature Cited

1. Rothrock HS. Phenol-formaldehyde. *United States Patent Application Publication*. 2,321,627, 1943.
2. Pizzi A. Handbook of Adhesive Technology. In: Pizzi A, Mittal KL, editors. *Natural Phenolic Adhesives II: Lignin*. New York: Marcel Dekker, 2003:1031.

3. Gardziella A, Pilato LA, Knop A. Phenolic Resins: Chemistry, Applications, Standardization, Safety and Ecology, 2nd ed. Heidelberg: Springer, 2000.
4. Netravali AN, Chabba S. Composites get greener. *Mater Today*. 2003;6:22–29.
5. Zakzeski J, Bruijnincx PCA, Jongerius AL, Weckhuysen BM. The catalytic valorization of lignin for the production of renewable chemicals. *Chem Rev*. 2010;110:3552–3599.
6. Kobayashi H, Fukuoka A. Synthesis and utilisation of sugar compounds derived from lignocellulosic biomass. *Green Chem*. 2013;15: 1740–1763.
7. Tejado A, Pena C, Labidi J, Echeverria JM, Mondragon I. Physicochemical characterization of lignins from different sources for use in phenol–formaldehyde resin synthesis. *Bioresour Technol*. 2007;98: 1655–1663.
8. Trosa A, Pizzi A. A no-aldehyde emission hardener for tannin-based wood adhesives for exterior panels. *Eur J Wood Wood Prod*. 2001; 59:266–271.
9. Devi A, Srivastava D. Cardanol-based novolac-type phenolic resins. I. A kinetic approach. *J Appl Polym Sci*. 2006;102:2730–2737.
10. Hahnenstein I, Hasse H, Kreiter CG, Maurer G. ^{1}H- and ^{13}C-NMR Spectroscopic Study of Chemical Equilibria in Solutions of Formaldehyde in Water, Deuterium Oxide, and Methanol. *Ind Eng Chem Res*. 1994;33:1022–1029.
11. Kowatsch S. Formaldehyde. In: Pilato L, editor. *Phenolic Resins: A Century of Progress*. Berlin: Springer, 2010:25–40.
12. Arts J, Rennen M, Heer C. Inhaled formaldehyde: evaluation of sensory irritation in relation to carcinogenicity. *Regul Toxicol Pharmacol*. 2006;44:144–160.
13. Huber GW, Iborra S, Corma A. Synthesis of transportation fuels from biomass: chemistry, catalysts, and engineering. *Chem Rev*. 2006;106:4044–4098.
14. Klemm D, Heublein B, Fink HP, Bohn A. Cellulose: fascinating biopolymer and sustainable raw material. *Angew Chem Int Ed*. 2005;44: 3358–3393.
15. Davda RR, Dumesic JA. Renewable hydrogen by aqueous-phase reforming of glucose. *Chem Commun*. 2004;1:36–37.
16. Davda RR, Shabaker JW, Huber GW, Cortright RD, Dumesic JA. A review of catalytic issues and process conditions for renewable hydrogen and alkanes by aqueous-phase reforming of oxygenated hydrocarbons over supported metal catalysts. *Appl Catal B*. 2005;56: 171–186.
17. Onda A, Ochi T, Yanagisawa K. Selective hydrolysis of cellulose into glucose over solid acid catalysts. *Green Chem*. 2008;10:1033–1037.
18. Daoutidis P, Marvin WA, Rangarajan S, Torres AI. Engineering biomass conversion processes: a systems perspective. *AIChE J*. 2013; 59:3–18.
19. Wu D, Fu R. Synthesis of organic and carbon aerogels from phenol–furfural by two-step polymerization. *Microporous Mesoporous Mater*. 2006;96:115–120.
20. Nielsen AT, Moore DW, Ogan MD, Atkins RL. Structure and chemistry of the aldehyde ammonias. 3. Formaldehyde-ammonia reaction. 1, 3, 5-Hexahydrotriazine. *J Org Chem*. 1979;44:1678–1684.
21. Richmond HH, Myers GS, Wright GF. The reaction between formaldehyde and ammonia. *J Am Chem Soc*. 1948;70:3659–3664.
22. Lytle CA, Bertsch W, McKinley M. Determination of novolac resin thermal decomposition products by pyrolysis-gas chromatography-mass spectrometry. *J Anal Appl Pyrolysis*. 1998;45:121–131.
23. Jacobs DE, Kelly T, Sobolewski J. Linking public health, housing, and indoor environmental policy: successes and challenges at local and federal agencies in the United States. *Environ Health Perspect*. 2007;115:976–982.
24. Simitzis J, Karagiannis K, Zoumpoulakis L. Influence of biomass on the curing of novolac-composites. *Eur Polym J*. 1996;32:857–863.
25. Sergeev VA, Shitikov VK, Nechaev AI, Chizhova NV, Kudryavsteva NN. Hydroxymethyl derivatives of phenols as curing agents for novolacs. *Polym Sci Ser B*. 1995;37:273–276.
26. Grenier-Loustalot M, Larroque S, Grenier P. Phenolic resins: 4. Self-condensation of methylolphenols in formaldehyde-free media. *Polymer*. 1996;37:955–964.
27. Aden A, Bozell J, Holladay J, White J, Manheim A. Top value-added chemicals from biomass. DOE Report PNNL-16983. 2004; PNNL-14808:1–66. Available at: http://chembioprocess.pnl.gov/staff/staff_info.asp, accessed on April 20, 2014.
28. Mwaikambo LY, Ansell MP. Cure characteristics of alkali catalysed cashew nut shell liquid-formaldehyde resin. *J Mater Sci*. 2001;36: 3693–3698.
29. Yan H, Yang Y, Tong D, Xiang X, Hu C. Catalytic conversion of glucose to 5-hydroxymethylfurfural over SO_4^{2-}/ZrO_2 and $SO_4^{2-}/ZrO^{2-}Al_2O_3$ solid acid catalysts. *Catal Commun*. 2009;10:1558–1563.
30. Zhao H, Holladay JE, Brown H, Zhang ZC. Metal chlorides in ionic liquid solvents convert sugars to 5-hydroxymethylfurfural. *Science*. 2007;316:1597–1600.
31. Yong G, Zhang Y, Ying JY. Efficient Catalytic System for the Selective Production of 5-Hydroxymethylfurfural from Glucose and Fructose. *Angew Chem Int Ed*. 2008;120:9485–9488.
32. Yuan Z, Xu CC, Cheng S, Leitch M. Catalytic conversion of glucose to 5-hydroxymethyl furfural using inexpensive co-catalysts and solvents. *Carbohydr Res*. 2011;346:2019–2023.
33. Cai SX, Lin CH. Flame-retardant epoxy resins with high glass-transition temperatures from a novel trifunctional curing agent: Dopotriol. *J Polym Sci Part A: Polym Chem*. 2005;43:2862–2873.
34. Pérez JM, Rodríguez F, Alonso MV, Oliet M. Time–temperature–transformation cure diagrams of phenol–formaldehyde and lignin–phenol–formaldehyde novolac resins. *J Appl Polym Sci*. 2011;119: 2275–2282.
35. Elavarasan P, Kondamudi K, Upadhyayula S. Kinetics of phenol alkylation with *tert*-butyl alcohol using sulfonic acid functional ionic liquid catalysts. *Chem Eng J*. 2011;166:340–347.
36. Um M, Daniel IM, Hwang B. A study of cure kinetics by the use of dynamic differential scanning calorimetry. *Compos Sci Technol*. 2002;62:29–40.
37. Freeman ES, Carroll B. The application of thermoanalytical techniques to reaction kinetics: the thermogravimetric evaluation of the kinetics of the decomposition of calcium oxalate monohydrate. *J Phys Chem*. 1958;62:394–397.
38. Kissinger HE. Reaction kinetics in differential thermal analysis. *Anal Chem*. 1957;29:1702–1706.
39. Ozawa T. A new method of analyzing thermogravimetric data. *Bull Chem Soc Jpn*. 1965;38:1881–1886.
40. Flynn JH, Wall LA. A quick, direct method for the determination of activation energy from thermogravimetric data. *J Polym Sci Part B: Polym Phys*. 1966;4:323–328.
41. Crane LW, Dynes PJ, Kaelble DH. Analysis of curing kinetics in polymer composites. *J Polym Sci Polym Phys Ed*. 1973;11:533–540.
42. Lee YK, Kim DJ, Kim HJ, Hwang TS, Rafailovich M, Sokolov J. Activation energy and curing behavior of resol-and novolac-type phenolic resins by differential scanning calorimetry and thermogravimetric analysis. *J Appl Polym Sci*. 2003;89:2589–2596.
43. Santos R, Souza AA, Paoli MD, Souza CM. Cardanol-formaldehyde thermoset composites reinforced with buriti fibers: Preparation and characterization. *Compos A*. 2010;41:1123–1129.
44. Pilato L. Phenolic resins: A century of progress. Springer Verlag, 2010.
45. Joseph S, Sreekala MS, Oommen Z, Koshy P, Thomas S. A comparison of the mechanical properties of phenol formaldehyde composites reinforced with banana fibres and glass fibres. *Compos Sci Technol*. 2002;62:1857–1868.
46. Joseph K, Varghese S, Kalaprasad G, Thomas S, Prasannakumari L, Koshy P, Pavithran C. Influence of interfacial adhesion on the mechanical properties and fracture behaviour of short sisal fibre reinforced polymer composites. *Eur Polym J*. 1996;32:1243–1250.

Manuscript received Apr. 24, 2014, and revision received Dec. 1, 2014.